Weichselian temperatures from geothermal heat flow data

Ilmo T. Kukkonen
Geological Survey of Finland, Espoo, Finland

Argo Jõeleht
Institute of Geology, University of Tartu, Tartu, Estonia

Received 16 October 2001; revised 20 May 2002; accepted 30 September 2002; published 20 March 2003.

[1] We report an analysis of geothermal heat flow density (HFD) in the Fennoscandian Shield and East European Platform showing a systematic variation with depth. The HFD data (1352 values) averaged in 25 m depth intervals and in $1° \times 2°$ latitude-longitude areas increase from ~35–40 mW m^{-2} in the first 500 m to ~45 mW m^{-2} at 1000 m, finally reaching ~50 mW m^{-2} between 1000 and 3000 m and deeper. We attribute this variation to long-term climatic changes in ground surface temperatures (GST) during the Weichselian (late Pleistocene) glaciation and the Holocene. Monte Carlo inversion was applied for determining ground surface temperature histories during the past 100,000 years, and the results indicate the lowest GST at time of the Last Glacial Maximum (~20,000 years B.P.), followed by an average warming of $8.0 \pm 4.5°$ at ~10,000 years B.P. *INDEX TERMS:* 1620 Global Change: Climate dynamics (3309); 1699 Global Change: General or miscellaneous; 3210 Mathematical Geophysics: Modeling; 9335 Information Related to Geographic Region: Europe; *KEYWORDS:* heat flow, geothermal gradient, paleoclimatology, Weichselian, Monte Carlo analysis, models

Citation: Kukkonen, I. T., and A. Jõeleht, Weichselian temperatures from geothermal heat flow data, *J. Geophys. Res.*, *108*(B3), 2163, doi:10.1029/2001JB001579, 2003.

1. Introduction

[2] We report results showing that Weichselian (late Pleistocene) paleotemperatures can be directly determined from geothermal heat flow data sets extending to depths of several kilometers. Heat flow density (HFD), determined as the product of thermal conductivity and temperature gradient in boreholes, is a major parameter characterizing the internal thermal regime of the Earth. A determined value of HFD is dependent on many factors, such as crustal heat production, heat flow from the mantle, surface topography, uplift, subsidence, erosion, sedimentation, lateral conductivity contrasts (channeling of heat flow), variations in the past ground surface temperature (paleoclimate), and convective heat transfer.

[3] Heat flow density values are usually not constant with depth. Vertical variation can be created by any of the above mentioned factors, and there are forward and inverse techniques to correct for these effects to obtain a steady state value of HFD [e.g., *Powell et al.*, 1988]. Measurements in Russian and German superdeep drill holes reaching depths of 5–12 km (in contrast to typical heat flow determinations in holes typically <1 km deep) have revealed considerable vertical variation in HFD which could not be explained completely by standard corrections [*Kremenetsky and Ovchinnikov*, 1986; *Popov and Berezyn*, 1993; *Popov et al.*, 1998a, 1998b, 1999a, 1999b; *NEDRA*, 1992; *Clauser et al.*, 1997; *Schellschmidt and Schulz*, 1991; *Pribnow and Schellschmidt*, 1998]. In addition to superdeep holes, anomalously low conductive heat flow values are reported in the uppermost 1 km in Karelia, NW Russia, and in the Urals [*Kukkonen et al.*, 1997a, 1998]. Authors have mostly attributed the observed vertical variation to either convective heat transfer [*Popov et al.*, 1998a, 1998b], a combined effect of postglacial uplift of lithosphere and convective heat transfer [*Popov et al.*, 1999a], or a combination of convective heat transfer, paleoclimate and structural effects [*Kukkonen and Clauser*, 1994].

[4] *Huang et al.* [1997] used the same Global Heat Flow Data Base of the International Heat Flow Commission of IASPEI [*Pollack et al.*, 1993] as we use in this paper, but they inverted a global set of data (data depths in the range 100–2000 m) for ground surface temperature (GST) variations during the last 20,000 years. Their inversion result suggests only a small average global warming (<1.5 K) at the Pleistocene/Holocene boundary, and an early Holocene warm period with 0.2–0.6 K above present temperatures, as well as small variations during the last 1000 years in agreement with proxy climate indicators. The small amplitudes in inverted GST changes by *Huang et al.* [1997] can be attributed to the averaging of data globally.

[5] In central Europe, the German KTB superdeep holes [*Clauser et al.*, 1997] show a systematic vertical variation in HFD with depth, attributed mainly to a paleoclimatic effect created by low GST values during the glaciation time (although the KTB site was never glaciated) and refraction of heat by conductivity contrasts. Heat transport by fluid

Copyright 2003 by the American Geophysical Union.
0148-0227/03/2001JB001579$09.00

flow is limited to the topmost 400 m of the drilled section [*Kohl and Rybach*, 1996]. In Canada, where the Wisconsin glaciation is analogous to the Weichselian in Europe, two deep holes have been analyzed. In Flin Flon, Manitoba, no obvious effect in HFD due to the Pleistocene paleoclimate could be detected in a 2.9 km deep hole [*Sass et al.*, 1971]. This was interpreted as either due to an unknown effect of comparable magnitude but opposite sign as the paleoclimatic effect, or due to inadequate models on Pleistocene paleoclimate. *Wang* [1992] analyzed the same data with inversion methods but could detect only a very mild warming effect (<1 K) at the end of the Pleistocene. *Mareschal et al.* [1999] investigated a 1.8 km deep hole in Sept-Iles, Quebec. Monte Carlo inversions for GST history indicated low temperatures (−5°C) during the Wisconsin glaciation followed by much warmer temperatures (+6°C) during early Holocene (5000–10,000 years B.P.) when the site was below sea level. The climatic correction of HFD determined at depths of <1000 m was determined as 4–5 mW m^{-2} only. This may be due to the strong Holocene marine effect. *Dahl-Jensen et al.* [1998] used Monte Carlo inversion for determining the surface temperatures on top of the Greenland ice sheet for the last 50,000 years using direct temperature measurements in boreholes through the ice sheet. The result indicates that Greenland temperatures at the Last Glacial Maximum (LGM, ∼18,000–22,000 years B.P.) were as much as 23 K below the present values.

[6] Given that vertical variation in HFD were common, it would have important implications on interpreting heat flow data sets for lithospheric purposes. For instance, a bias of 20 mW m^{-2} in the surface HFD value yields an error of 300–400°C in calculated temperatures at 50 km depth. It is therefore relevant to understand the major factor(s) behind such a variation and to correct the data accordingly.

[7] We investigate the vertical variation in HFD in the Fennoscandian Shield (FS) and the East European Platform (EEP), where a large number of deep geothermal measurements in addition to superdeep hole data are available. We aim at finding out whether vertical variation occurs generally, and whether it could be attributed to long-term climatic changes in the timescale of glaciations [cf. *Dahl-Jensen et al.*, 1998]. Geothermally, the area does not show large areal variations in HFD [*Hurtig et al.*, 1992]. Precambrian bedrock outcrops in the FS, but it is covered by a thin (mostly <2 km thick) layer of sediments in the platform area. As a whole, the study area is relatively homogeneous and has not been influenced by major tectonothermal events for hundreds of millions of years.

2. Vertical Variation in Heat Flow Density in the Fennoscandian Shield and East European Platform

[8] We utilize here a data set taken from the Global Heat Flow Data Base of the International Heat Flow Commission of IASPEI [*Pollack et al.*, 1993] supported by national data sets from Finland [*Järvimäki and Puranen*, 1979; *Kukkonen*, 1988, 1989; *Kukkonen and Järvimäki*, 1992] and Estonia [*Urban and Tsybulia*, 1988; *Urban et al.*, 1991; *Moiseenko and Chadovich*, 1992; *Jõeleht and Kukkonen*, 1996; *Jõeleht*, 1998] as well as measurements in eastern Karelia [*Kukkonen et al.*, 1998] and central Kola Peninsula [*Kukkonen et al.*, 1997b]. The complete data set comprises

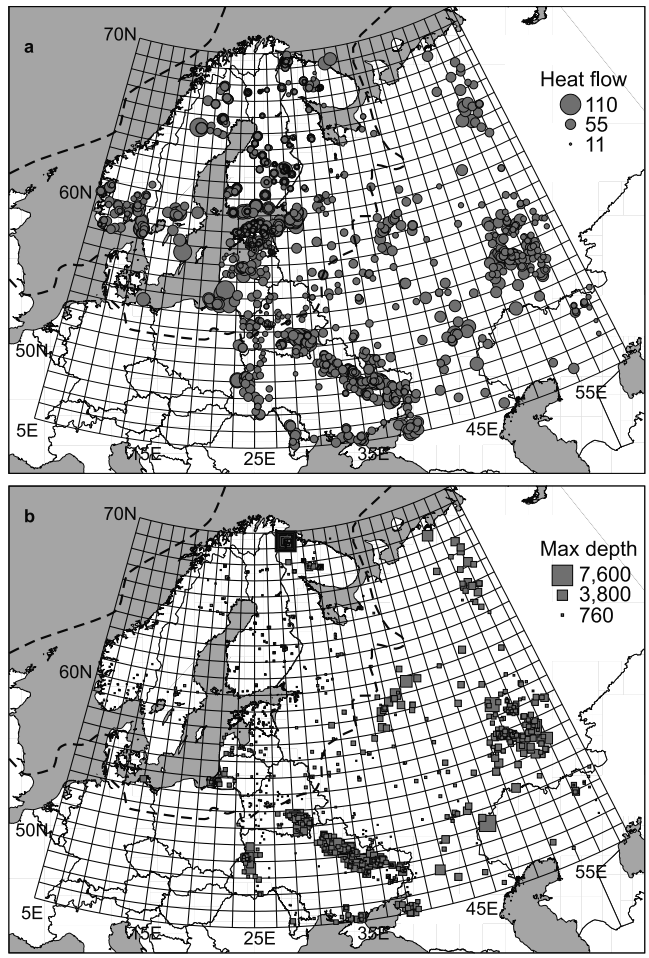

Figure 1. (a) Lateral distribution of HFD values and (b) depth of HFD measurements. The maximum extent of Late Weichselian glaciation [*Svendsen et al.*, 1999] is indicated with a dashed line.

1352 values of HFD. Most of the data (∼1000 values) come from the top 1 km, while only 71 heat flow values are reported with interval average depths >2 km. The deep data (>3 km) values represent both EEP and FS (Figure 1).

[9] The data entries comprise of HFD values determined as products of vertical temperature gradient in a given depth interval (calculated from measured temperature-depth logs) and thermal conductivities measured in laboratory from drill core samples or drill chips. Because of the large number of original research groups responsible of the data the determination errors may have varied. For instance, the IHFC Global heat flow catalogue does not report errors of HFD determination for each borehole. Typically, HFD is determined with an error of the order of ±5 mW m^{-2}, and the exact values depend on the quality of the original temperature log (number and depth interval of temperature readings used, calibration of instrument and thermal condition of borehole) as well as the measurements of thermal conductivity. Original temperature logs are given only occasionally in the data sources used in this study, mostly in the Finnish and Estonian national data sets cited above.

[10] The unprocessed data show relatively large scatter of values (Figure 2a), and it is difficult to recognize any

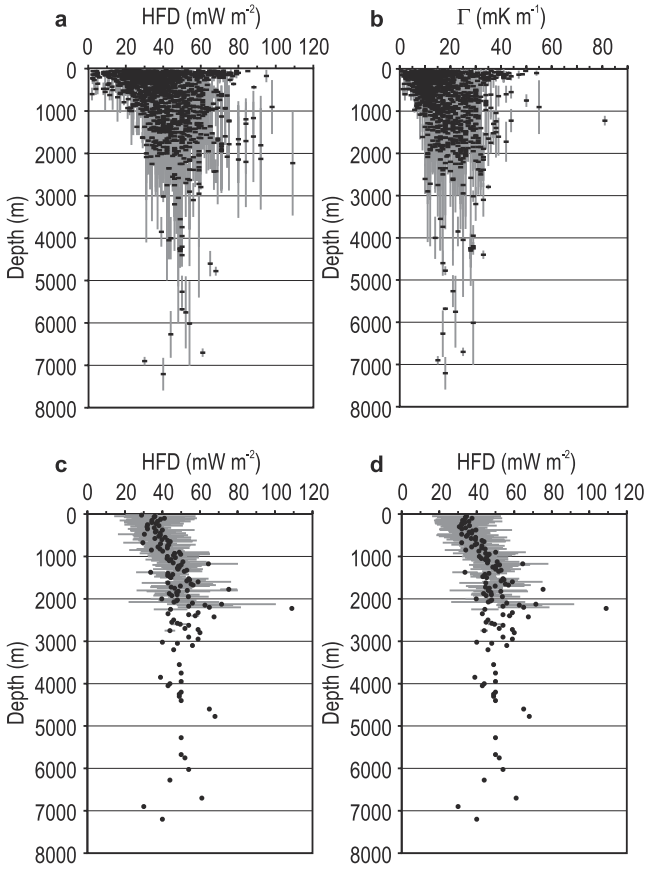

Figure 2. (a) Raw HFD versus depth data with the upper and lower depths of measurements indicated with vertical bars, (b) temperature gradients versus depth, (c) HFD and its standard deviation versus depth after averaging over 25 m depth intervals, and (d) as in Figure 2c but after averaging over 25 m depth and $1° \times 2°$ latitude-longitude windows.

systematic vertical variation. The blurring effect of data scatter can be reduced by averaging. We used 25 m for depth interval and $1° \times 2°$ for latitude-longitude areas as averaging windows which proved out to yield reasonable smoothing without any apparent loss of information. The results are not very sensitive for the window size used in averaging. Also other values were applied but the results did not essentially change. Data averaged over 25 m depth intervals and $1° \times 2°$ latitude-longitude areas show a distinct trend of increasing HFD with depth from ~35–40 mW m^{-2} at 0–500 m to ~50 mW m^{-2} at depths of 3000 m and deeper, being equal to >40% increase in HFD. (Figures 2b and 2c and Table 1). The result indicates that the vertical variation in HFD is a common feature in the study area and not limited to superdeep holes alone.

3. Factors Influencing Vertical Variation in HFD

[11] In the study area, the detected vertical variation in HFD could be attributed to many factors locally, but as the variation is present on a continent-wide data set we want to seek for common, generic processes. This does not imply that there should be only one factor for the vertical HFD variation, but we consider such a case most probable.

Table 1. Average HFD With Depth in the FS and EEP[a]

Depth, m	HFD, mW m^{-2}	SD, mW m^{-2}	*N*
50	34.5	18.4	15
75	34.0	15.1	24
100	37.4	16.2	30
125	33.4	15.4	36
150	32.4	15.2	41
175	35.8	17.9	32
200	33.6	16.1	23
225	32.1	14.2	26
250	32.1	13.3	30
275	36.2	14.5	31
300	30.7	10.0	18
325	34.1	11.7	25
350	32.0	12.0	28
375	39.5	19.3	16
400	37.7	12.9	20
425	35.9	10.9	17
450	37.3	10.1	22
475	32.0	13.0	15
500	35.0	16.6	16
525	34.5	14.7	15
550	39.4	16.9	20
575	37.0	11.0	17
600	39.3	15.4	16
625	42.8	15.2	22
650	43.9	11.5	18
675	31.9	10.1	6
700	40.0	8.1	10
725	39.1	12.7	8
750	42.8	12.1	19
775	37.3	3.9	4
800	42.6	11.3	11
825	44.5	11.5	8
850	34.2	11.3	10
875	41.1	10.8	9
900	50.0	16.1	13
925	44.7	17.4	12
950	46.6	14.0	11
975	45.9	12.8	7
1000	41.4	9.4	16
1025	45.2	11.5	8
1050	42.5	7.4	8
1075	44.6	12.2	5
1100	46.0	8.9	10
1125	50.9	11.9	8
1150	45.8	7.6	4
1175	64.5	13.7	4
1200	52.1	16.3	5
1225	50.1	12.1	7
1250	48.6	10.6	9
1275	50.0	7.4	6
1300	50.1	13.5	10
1325	53.0	5.0	2
1350	51.6	8.7	8
1375	33.7	6.8	4
1400	46.5	9.7	9
1425	44.3	8.0	8
1450	44.2	5.9	7
1475	43.3	6.6	4
1500	45.3	5.6	10
1525	54.0	8.6	3
1550	54.5	7.5	4
1575	53.0	–	1
1600	59.0	16.1	6
1625	44.8	14.1	6
1650	55.3	10.2	4
1675	56.9	12.0	5
1700	49.8	15.6	9
1725	44.7	9.2	3
1750	46.7	7.2	6
1775	75.3	–	1
1800	46.1	20.6	4
1825	52.8	14.5	3
1850	47.6	5.6	5

Table 1. (continued)

Depth, m	HFD, mW m^{-2}	SD, mW m^{-2}	N
1875	43.7	6.3	3
1900	47.8	11.0	6
1925	45.0	7.0	2
1950	53.7	9.5	6
2000	39.8	5.8	4
2025	48.0	8.3	3
2050	47.3	1.7	3
2075	46.1	19.7	3
2100	56.0	–	1
2125	71.5	20.5	2
2150	62.7	12.3	3
2175	54.0	–	1
2200	65.0	13.7	3
2225	109.0	–	1
2250	44.3	7.3	3
2325	59.0	–	1
2350	43.0	0.0	2
2375	54.0	–	1
2400	57.5	1.5	2
2425	67.5	0.5	2
2500	46.0	–	2
2550	45.0	–	1
2575	48.0	–	1
2600	49.5	3.5	2
2625	54.0	–	1
2700	52.0	–	1
2725	59.0	–	1
2750	44.0	2.0	2
2800	60.0	–	1
2900	54.0	–	1
2950	59.0	–	1
3025	40.0	–	1
3050	48.0	–	1
3100	56.0	–	1
3200	46.0	–	1
3550	49.0	–	1
3750	50.0	–	1
3850	39.0	–	1
3950	50.0	–	1
4000	44.0	–	1
4050	43.0	–	1
4200	50.0	–	1
4250	49.0	–	1
4300	49.0	–	1
4400	50.0	–	1
4600	65.0	–	1
4775	68.0	–	1
5275	50.0	–	1
5675	50.0	–	1
5750	52.0	–	1
6025	54.0	–	1
6275	44.0	–	1
6700	61.0	–	1
6900	30.0	–	1

[a]Depth corresponds to the center of each 25 m long depth interval.

[12] Structural factors, such as thermal conductivity and heat production rate contrasts are not able to produce vertical increase in HFD with depth, because steady state heat flow density is an integral of mantle heat flow and heat generated in crustal layers beneath the depth of measurement. Uplift, erosion, subsidence, sedimentation or topographic effects are not relevant from the point of view of heat flow variations in the area because of its old geological age, stabilized character, and subdued topography.

[13] Convective heat transfer by fluid flow is capable of considerable modification of the conductive heat flow field, given that a sufficient driving force is available and rock hydraulic permeability exceeds critical values [e.g., *Lewis and Beck*, 1977; *Smith and Chapman*, 1983; *Drury et al.*, 1984; *Clauser and Villinger*, 1990; *Van der Kamp and Bachu*, 1989; *Beck et al.*, 1989; *Kukkonen*, 1995]. Downward flow (recharge) should be observed as an increase of apparent geothermal gradient and heat flow with depth and upward flow (discharge) as a decrease, respectively. Downward migration of fluids has been postulated for the Kola and the Vorotilovsk superdeep hole sites [*Popov et al.*, 1998a, 1999a]. Such flow systems may exist locally, but it is highly implausible that they would prevail allover in the FS and EEP comprising diverse hydrogeological environments. Moreover, ubiquitous downward flow of water in the upper crust in such a large area should also produce recognizable demonstrations of discharge, which however, are not reported. It is plausible that a part of the variation in the HFD data is due to heat transfer by local groundwater flow systems, but we do not consider any realistic flow systems to be capable of creating such a systematic vertical variation in HFD.

[14] Long-period paleoclimatic variations in ground surface temperatures (GST) are phenomena on a continental scale at least and could easily provide effects influencing our study area as a whole. Assuming that the detected vertical variation is due to paleoclimatic factors, i.e., downward diffusion of GST changes, the depth scale of the detected variation ($\sim$2km, Figure 2) implies climate changes in the timescale of glaciations ($\sim$100,000 years) [e.g., *Birch*, 1948; *Beck*, 1977]. Even in the presence of convective heat transfer by groundwater flow, conductive diffusion effects cannot be completely ''washed out'' by convection [*Kohl*, 1998].

4. Monte Carlo Inversion for Ground Surface Temperature History: Model Resolution and Inversions of Synthetic Data

[15] There is no unique solution for the inverse problem of finding a GST history from a vertical profile of HFD values. The difficulty of determining GST history is further accentuated by noise. The Monte Carlo inversion applied here is a method designed for sampling possible models in the a priori model space and testing the models according to preset requirements for rejecting or accepting them in the a posteriori model space [*Mosegaard and Tarantola*, 1995; *Sen and Stoffa*, 1995].

[16] Heat flow density differences between the measured values and an assumed steady state condition were inverted to GST using a homogeneous half-space model of the subsurface. Since we do not know the value of undisturbed surface heat flow density, it is also included in the inversion as an unknown parameter in addition to ground surface temperatures in the past. Heat flow density differences are transformed into temperature gradient differences by dividing with thermal conductivities also reported in the data sources. The perturbation of temperature gradient $\Delta\Gamma$ at depth z due to N step changes of surface temperature ΔT for a time period $t_n < t < t_{n+1}$ is [*Carslaw and Jaeger*, 1959; *Powell et al.*, 1988]

$$\Delta\Gamma(z,t) = \sum_{n=1}^{N} -\Delta T_{t_n} \cdot \left(\frac{\exp(-z^2/4at_{n+1})}{\sqrt{\pi a t_{n+1}}} - \frac{\exp(-z^2/4at_n)}{\sqrt{\pi a t_n}} \right), \tag{1}$$

where a is the thermal diffusivity.

[17] To run an inversion, a random GST history is first drawn within a given a priori range. A conservative model with only small (0 ± 2 K) GST variations is assumed for all time intervals in inversion and the corresponding temperature gradient disturbance is calculated, as well as the misfit E between data and model gradients [*Mosegaard and Tarantola*, 1995]:

$$E = \frac{1}{2}\sum_{i=1}^{N}(\Delta\Gamma_{i\,\mathrm{calc}} - \Delta\Gamma_{i\,\mathrm{obs}})^2. \quad (2)$$

Next, the temperature for one of the time periods, or the steady state surface HFD, is randomly changed using step lengths which at maximum may equal the given a priori ranges (±2 K and ±10 mW m^{-2}), and the corresponding temperature gradient disturbance is calculated again. If the misfit E_{new} of the new model is smaller than the misfit E_{old} of the previous model, the change is accepted. In case the misfit increases, the Metropolis rule [*Mosegaard and Tarantola*, 1995] is applied which still under certain conditions allows acceptance of this change. Namely, the acceptance probability for this case is

$$P_{\mathrm{accept}} = \exp\left(-\frac{E_{\mathrm{new}} - E_{\mathrm{old}}}{s^2}\right), \quad (3)$$

where s^2 is the noise variance of data, which is assumed to be Gaussian. The noise variance is a critical inversion parameter. Too high values may lead to acceptance of all changes, whereas too small values may result in getting stuck in local minima and provoking amplification of noise in the solution. Noise variance values corresponding to data standard deviations of 2–5 mK m^{-1} were applied.

[18] The time intervals used in the inversion increase with increasing time B.P. due to decreasing resolution with time. In the present case we applied a factor of 1.5 for increasing the length of consecutive time periods, with the total number of 24 time periods extending to 167,000 years B.P. In addition, we also calculate the preobservational mean (POM) GST, i.e., the long-term mean temperature before the 24th time period.

[19] In the random walk algorithm, only one parameter (GST of a time period or the steady state HFD value) is changed at a time, the corresponding gradient profile is calculated, and the model is tested against observations. We required 50,000 accepted changes before a new model was added to the a posteriori distribution. This ensured that the a posteriori models were independently sampled. The number of models in the a posteriori distribution was chosen empirically. About 1000 models were needed to achieve smooth distributions of temperature values for each time step/heat flow in the a posteriori distribution. Thus the present results are based on ~50 million forward calculations of the models. For the calculations we applied a source code used by *Mareschal et al.* [1999] but modified by us for the present study.

[20] Because of the diffusive nature of heat conduction, the amplitude of temperature gradient perturbations decreases with increasing time and depth. This results in decreasing resolution with increasing event time before present. We have basically two problems: First, whether our data are able to carry any signal from the past GST events in the time period investigated, and second, whether the applied inversion method is able to provide any resolution of the events in inverting the (noisy) data.

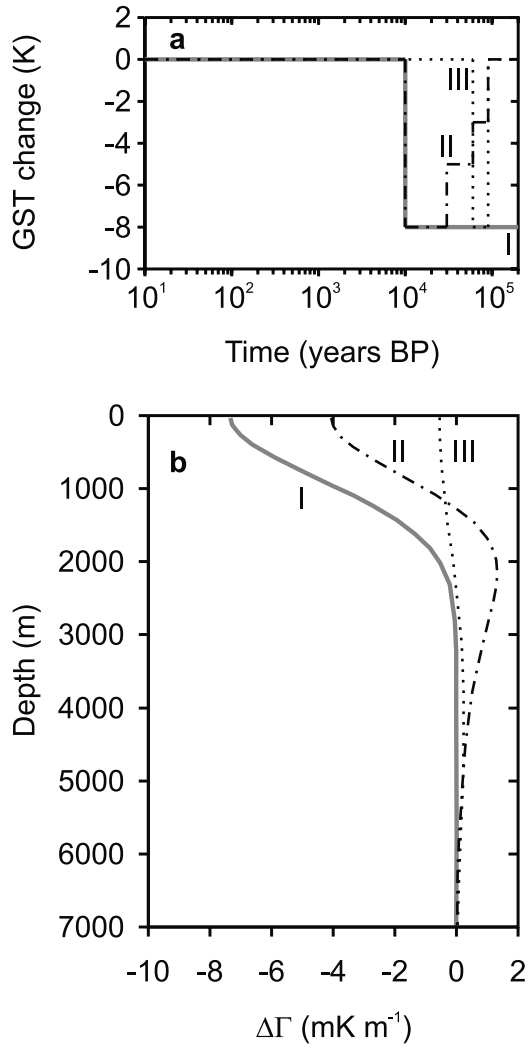

Figure 3. Theoretical disturbances on the geothermal gradient by three different GST variations during the Weichselian period calculated from equation (1). Model I, temperature increase of 8 K at 10,000 years B.P., i.e., a pure deglaciation effect; model II, gradual cooling during Weichselian until the LGM (temperature difference −3 K from 90,000 years B.P. to 60,000 years B.P., −5 K from 60,000 to 30,000 years B.P., −8 K from 30,000 to 10,000 years B.P.), followed by 8 K warming at 10,000 years B.P.; and model III, a cold period during Early Weichselian (−8 K, 90,000–60,000 years B.P.). Diffusivity is 1.2×10^{-6} m^2 s^{-1}.

[21] The existence of a temperature gradient signal from the Weichselian GST variations is demonstrated in Figure 3 with three types of synthetic models. Theoretical gradient disturbance due to a pure deglaciation effect (Figure 3, model I, temperature increase of 8 K at 10,000 years B.P. from an initial steady state condition) disappears at ~2.5 km. On the other hand, a cold period lasting for most of Weichselian and peaking before the Holocene (Figure 3, model II; −8 K at 10,000–30,000 years B.P., −5 K at

30,000–60,000 years B.P., and −3 K at 60,000–90,000 years B.P.) shows a much deeper extent of the gradient disturbances, with the maximum at the depth of ~2.1 km (maximum temperature disturbance would be at 1.3 km), and the anomaly remains above 0.5 mK m^{-1} to ~4 km depth. The third theoretical variant (Figure 3, model III) shows an Early Weichselian cold period of −8 K between 90,000 and 60,000 years B.P. The gradient disturbances due to this event are smaller than 0.5 mK m^{-1}.

[22] We can conclude that deep HFD data are able to carry a major signal produced by GST variations during the Late and Middle Weichselian times (<60,000 years B.P.) but there would be only a relatively small signal from the Early Weichselian (>60,000 years B.P.).

[23] Comparison of inversions with noise-free (Figure 4, left) and noise-added (Figure 4, right) synthetic data are shown in Figure 4. The added noise is Gaussian random noise with a standard deviation of 2.0 mK m^{-1}, and it corresponds to a typical HFD determination error of ±5 mW m^{-2}. The theoretical gradient variations were included at 25 m depth intervals and the profile extended to 7 km. These values also correspond to our real data compilation. Inversions of noise-free data return the original synthetic models very well for the pure deglaciation model (Figure 4a), as well as for the model with gradual cooling during the Weichselian (Figure 4c), but model resolution is poor for the Early Weichselian event (Figure 4e). Even in the presence of noise the inversion yields correct results for the pure deglaciation model (Figure 4b) and the model with gradually cooling GST's during the Weichselian (Figure 4d).

[24] The influence of the depth extent of data on inversion results is demonstrated in Figure 5, where the synthetic noise-added data of Figure 4d were cut to maximum depths of 2 and 1.5 km. Data extending to 2 km are still able to yield reasonably good inversion results on Late Weichselian GST history, whereas data cut to 1.5 km underestimate the temperature amplitude and the time of the major warming event at the Pleistocene-Holocene boundary.

[25] Quite expected, the most recent past (<100 years B.P.) is not ideally solved by inversion of noise-added data (Figures 4b, 4d, and 4e). We attribute this to the applied relatively dense discretization of the time axis for the recent part and the 25 m depth intervals in gradient values. Therefore the uppermost 150 m which best respond to the recent times (<100 years B.P.) are represented by only a few data points, and the results may be seriously influenced by the added random noise. However, we consider this effect less important for the primary interest of this paper, the Weichselian GST variations.

5. Inversion Results of HFD Data

[26] In steady state conditions heat flow density decreases with depth by the amount of heat that is produced by decay of radioactive elements in the overlaying rocks. The effect of heat production was removed from the averaged vertical HFD profiles using a heat production rate value of 1×10^{-6} W m^{-3}, probably representative of the upper crust. In case there was no thermal conductivity data given in the database, we used an average value (2.6 W m^{-1} K^{-1}) calculated over the whole data set. We used a thermal diffusivity value of 1.2×10^{-6} m^2 s^{-1}.

[27] Regardless of the noisy data, inversion results show a distinct GST variation. Already the inversion of nonaveraged raw data indicates a cold period at the end of Pleistocene (Figure 6). Timing the end of the cold period is not very sharp, and it extends from 15,000 years B.P. to ~4000 years B.P. We attribute this to the large scatter of the nonaveraged data. The high POM temperatures are caused by data points at depths >6000 m with relatively low HFD values (Figure 2). These few data points may be seriously influenced by noise and local geological circumstances.

[28] After averaging the data over depth and latitude-longitude windows, the scattering is significantly reduced and the end of the cold period is more sharply confined in inversion at ~10,000 years B.P. (Figure 7). The inversion indicates a gradual cooling through the Weichselian until the Last Glacial Maximum, followed by an average warming of 8.0 ± 4.5 K. The inverted Middle and Late Weichselian low temperatures are still within the reasonably well resolved time periods of deep temperature gradient data. However, the Early Weichselian temperatures and the POM estimate (3 ± 3.5 K above present) should not be emphasized too strongly due to same arguments as in inverting the raw data (Figure 6).

[29] The inversion gives very few details for the Holocene period, although there are GST variations suggesting warmer temperatures during Holocene and even a recent warming effect, but these are within model uncertainties (one standard deviation of a posteriori temperatures). The result can be attributed to relatively small climatic variations during the Holocene, but also to customs in reporting HFD data. Researchers usually do not report HFD by several depth intervals in a borehole, especially not from the shallow parts of holes which are often ignored completely, and therefore the Holocene signal is not well represented in the HFD data. It is also much smaller in amplitude in comparison to the Weichselian effect and therefore easily lost in the noise and further smoothed out in the averaging. Nevertheless, the Holocene signal can be observed locally in subsets of the present data compilation. For example, the Estonian HFD data [*Urban and Tsybulia*, 1988; *Urban et al.*, 1991; *Moiseenko and Chadovich*, 1992; *Jõeleht and Kukkonen*, 1996; *Jõeleht*, 1998], which come from shallow depths (mostly <400 m) and are mostly reported with short depth intervals (tens of meters), show an increase of average values from 20 mW m^{-2} at depths <50 m to ~35 mW m^{-2} at depths deeper than 200 m. The inversion of these data clearly indicates the Little Ice Age (seventeenth century) and recent warming during the last 100–150 years (Figure 8). The inversion result is consistent with direct air-temperature observations [*Jaagus*, 1998], which started in 1828, but also with climate reconstruction based on proxy data (first day of ice breakup in the Tallinn port and in North Estonian rivers, and the first day of rye harvest) going back to 1600 A.D. [*Tarand and Nordli*, 2001].

6. Discussion

[30] The present data are not sufficiently numerous for an investigation of subareas within the FS and EEP to reveal possible areal trends in the vertical HFD variation and GST history. Although the data from different latitudes seem to follow the same trends with depth, there are data gaps in

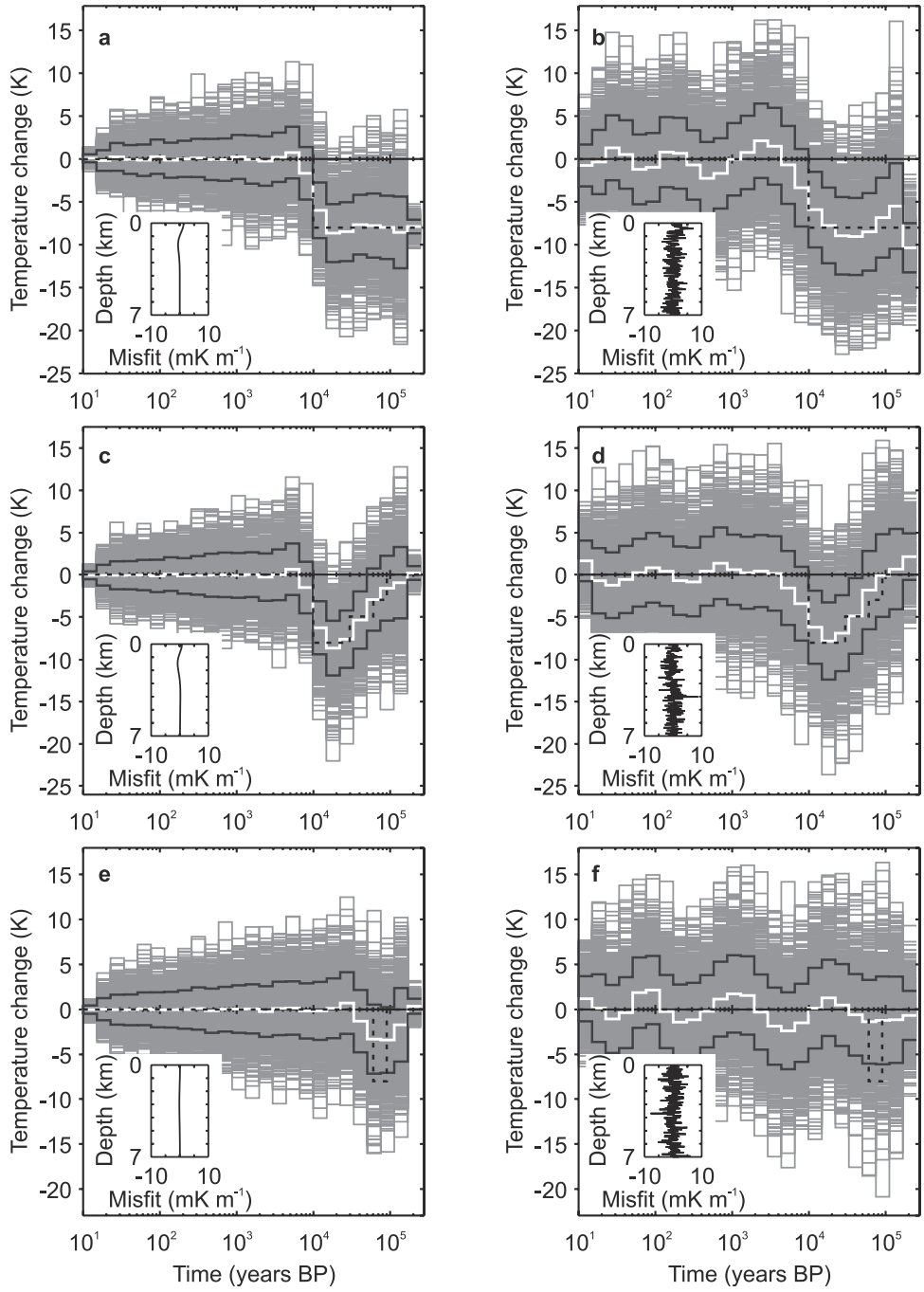

Figure 4. Inversions of synthetic data, which were generated using equation (1). All accepted a posteriori models and their temperatures (grey lines), the average temperature history (white line), and one standard deviation (black lines) are shown. The lengths of consecutive time periods in the inversion increase by a factor of 1.5. (left) Inversions of noise-free data and (right) noise-added data (Gaussian random noise with a standard deviation of 2.0 mK m^{-1}) are shown. The synthetic GST histories (indicated with dashed lines) are identical to those in Figure 3: (a and b) model I; (c and d) model II; and (e and f) model III. The so-called preobservational mean (POM) temperature is presented as the temperature of the last time period. The noise-free data were inverted with noise variance $s^2 = 1 \times 10^{-8}$ and the noise-added data with $s^2 = 4 \times 10^{-6}$ (equation (3)). They correspond to data standard deviations of 0.1 and 2 mK m^{-1} in gradient and to 0.25 and 5 mW m^{-2} in HFD, respectively (assuming thermal conductivity of 2.5 W m^{-1} K^{-1}). The insets indicate misfits, i.e., differences between calculated and observed data in terms of temperature gradient.

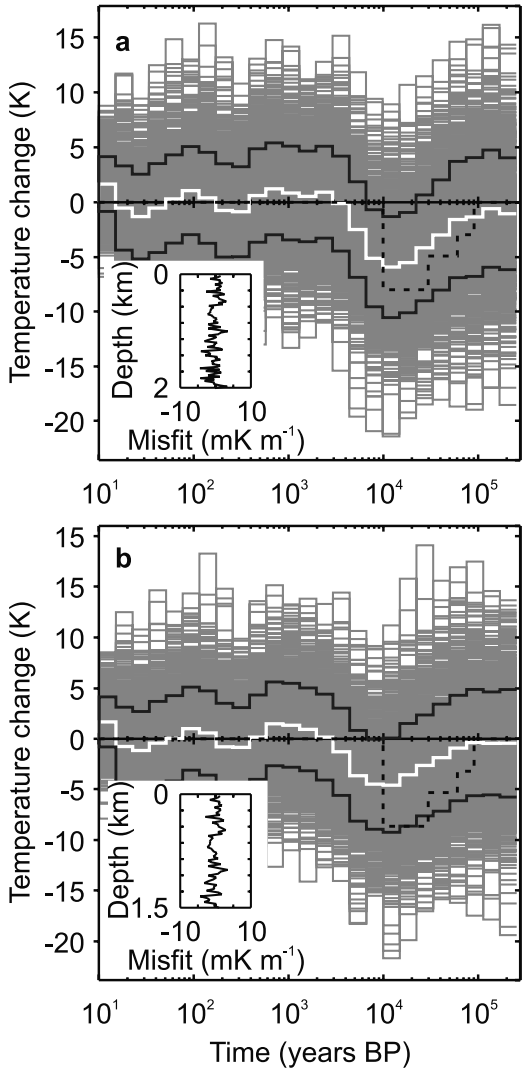

Figure 5. Inversion of synthetic noise-added data (Figure 3, model II), also inverted in Figure 4d, but the data depth cut at (a) 2.0 and (b) 1.5 km. The results demonstrate the loss of information when shallow data are used.

depth, which prevent the inversion of the glaciation signal properly.

[31] In a single borehole, the vertical variation in HFD may be difficult to interpret because of many factors simultaneously influencing the thermal regime. Usually very little information exists on the surrounding structures, as well as their thermal and hydraulic properties. Interpretation of HFD variations in a single hole is therefore a complicated problem and the number of free parameters may be too big. A single deep-hole result may differ from a joint inversion of a large group of holes, as is commonly observed in paleoclimatic inversion studies using borehole temperature logs [e.g., *Shen et al.*, 1995; *Harris and Chapman*, 2001].

[32] In the FS and EEP area, the vertical variation can be considered established, but we are not able to extend this conclusion to other areas due to lack of analysis, and particularly due to lack of deep borehole data.

[33] In the present study, the obtained a posteriori GST histories indicate a significant average warming of ~8.0 ±

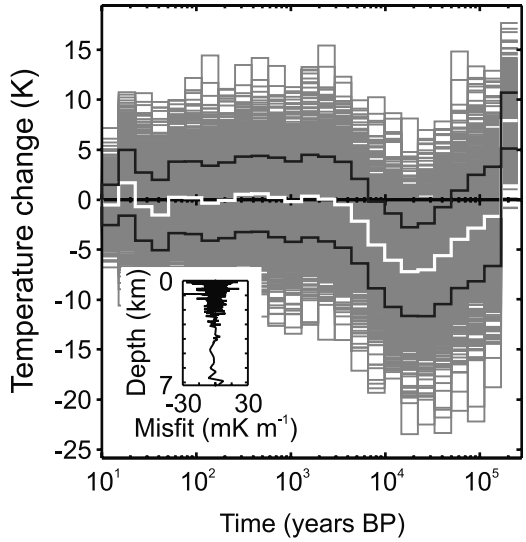

Figure 6. GST history for the past 100,000 years in the Fennoscandian Shield and East European Platform inverted from raw HFD data at 0–7000 m in Figure 2a. The applied noise variance $s^2 = 25 \times 10^{-6}$ corresponds to a data standard deviation of 5 mK m^{-1} or 13 mW m^{-2} assuming average thermal conductivity. The initial a priori model space assumed almost no temperature changes in the past (0 ± 2 K for each time step). In the random walk, the temperatures were then allowed to change within ±2 K of the previous model values. The effect of heat production was removed from the data assuming a value of 1×10^{-6} W m^{-3}. The obtained a posteriori steady state surface HFD estimate is 43.5 ± 1.0 mW m^{-2}.

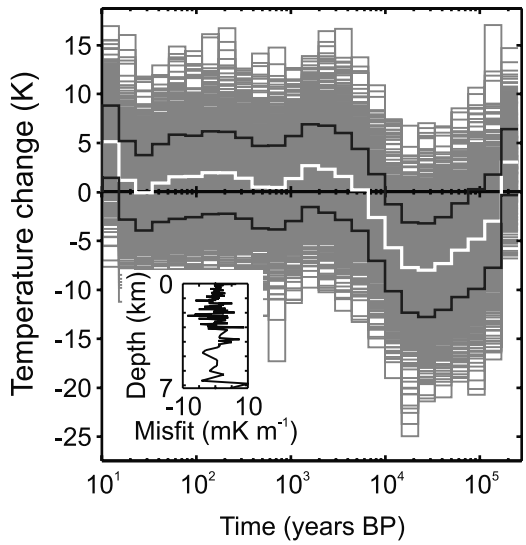

Figure 7. GST history as in Figure 6 but based on HFD data averaged over 25 m depth intervals and 1° × 2° latitude-longitude windows (Figure 2d). The applied noise variance $s^2 = 4 \times 10^{-6}$ corresponds to a temperature gradient standard deviation of 2 mK m^{-1}, and other parameters were the same as in Figure 6. The obtained a posteriori steady state surface HFD estimate is 49.7 ± 0.4 mW m^{-2}.

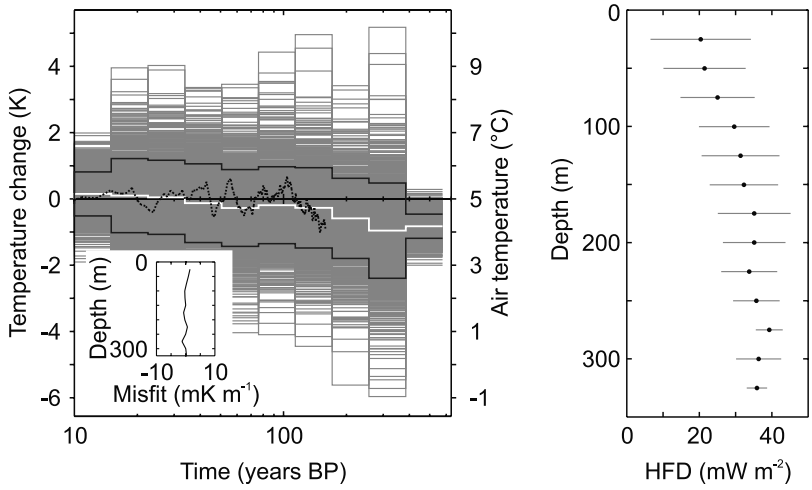

Figure 8. (right) Vertical increase of average HFD in Estonia (adapted from *Jõeleht* [1998]) can be explained (left) with the Little Ice Age and 1 K GST increase during 100–150 years B.P. The meteorological air temperatures (dotted line) are from *Jaagus* [1998].

4.5 K (1 standard deviation) from the LGM to Holocene in a good general agreement with common geological knowledge on climate warming at the Pleistocene/Holocene boundary. Only the northwestern and western parts of the study area were glaciated during the LGM [*Svendsen et al.*, 1999]. In Europe, the glaciation extended to about latitude 50°N, but it did not reach the Urals and extended only to about longitude 45–50°E in northern Russia. During the Early and Middle Weichselian glaciation maxima the Urals were covered by an ice sheet north of about 65°N. There were several cold climatic periods alternating with less cold interstadials during the Weichselian, but the general trend was a cooling from the EEM interglacial through the Weichselian until the Last Glacial Maximum, also suggested by inversion results in the present study. Anyway, the ice cover was not continuous either regionally nor temporally, and rapid fluctuations in ice sheet extent have taken place even at times close to the LGM [*Lunkka et al.*, 2001].

[34] The southern limit of continuous permafrost in Europe at the LGM time followed approximately the parallel 50°N with a permafrost temperature of −3°C (present GST about +6°C) [*Frenzel et al.*, 1992]. Permafrost thickness is estimated to have increased toward north from ∼200 m at 50°N to over 800 m on the (present) Arctic Sea coast in ice free areas, where ground temperatures have been as low as −10°C (present GST less than +2°C) [*Frenzel et al.*, 1992; *Baulin and Danilova*, 1984]. Our inversion result, suggesting that the average temperature difference between present and the LGM time was 8.0 ± 4.5 K, is in agreement with these data.

[35] While ice-free areas have experienced low temperatures during the Weichselian, ground temperatures beneath a glacier may have been substantially higher at the same time. The basal ice sheet temperatures are controlled by ice thickness, ice sheet surface temperature, accumulation rate, horizontal advection of ice, heat produced by internal friction of ice, roughness of basal topography and the basal heat flow from below the glacier [*Paterson*, 1994; *Siegert and Dowdeswell*, 1996]. For the most part the base of a thick glacier is at melting conditions and the temperature corresponds to the pressure-melting temperature. For pure ice it is −0.9°C for 1 km thick, and −1.7°C for a 2 km thick glacier, respectively [*Paterson*, 1994]. Most of the glacial corrections of HFD are based on the assumption of pressure-melting temperature beneath the ice [*Beck*, 1977; *Jessop*, 1971; *Kukkonen*, 1987; *Balling*, 1995] but do not consider the influence of cold ice-free periods. Assumption of pressure-melting temperatures also leads to a glacial correction which decreases toward north because the GST difference between present and the glaciation time decreases.

[36] It can be expected that areas which were covered the longest times by ice would have experienced higher average ground temperatures than those mostly outside the glacier. This would imply that, for instance, in Fennoscandia in the area of maximum ice thickness (the Bothnian Bay area in Finland and Sweden), vertical HFD variation would be smaller. There are not sufficient data to verify this, but the conclusion is supported by the apparent lack of a significant vertical variation in HFD in the Siljan, western Sweden, superdeep hole [*Balling et al.*, 1990], situated close to the Fennoscandian ice divide, and the detailed heat transfer modeling in a case from Outokumpu, eastern Finland, suggesting GST values of −1 to −2°C during the Weichselian [*Kukkonen and Šafanda*, 1996]. The very low HFD data reported from eastern Karelia, northwest Russia, which was most of the Late Weichselian time outside of, but close to the Fennoscandian ice sheet [*Kukkonen et al.*, 1998], also support such a model.

7. Conclusions

[37] A major result here is that geothermal HFD data sets can be applied for paleoclimatic reconstructions in the timescale of Late-Middle Weichselian (to ∼60,000 years before present) and they provide a direct, although noisy source of paleotemperature information. The vertical variation in HFD in the Fennoscandian Shield and East European Platform can be attributed to the major climate change at the Pleistocene-Holocene boundary, and our inversion result

suggests an average warming of 8.0 ± 4.5 K from the LGM time. Further, the present results indicate that the paleoclimatic correction of HFD data for the Weichselian effects may have been underestimated in the study area. We propose an average correction of +15 mW m^{-2} at 500 m depth, and +5 mW m^{-2} at 1000 m, respectively. The inversion yields a value of the steady state surface HFD for the study area as 49.7 ± 0.4 mW m^{-2}.

[38] **Acknowledgments.** We are grateful to J.-C. Mareschal for the copy of his Monte Carlo inversion code, to J. Jaagus for providing the air temperature data in Estonia, and to two anonymous reviewers for their comments on the manuscript. This investigation was partly financed from the Estonian research grant TBGGL0550.

References

Balling, N., Heat flow and thermal structure of the lithosphere across the Baltic Shield and northern Tornquist Zone, *Tectonophysics*, *244*, 13–50, 1995.

Balling, N., G. Lind, O. Landström, K. G. Eriksson, and D. Malmqvist, Thermal measurements from the deep Gravberg-1 well, *R, D&D Rep. U(G) 1990/57*, 13 pp., Swed. State Power Board, Vattenfall, 1990.

Baulin, V. V., and N. S. Danilova, Dynamics of Late Quaternary Permafrost in Siberia, in *Late Quaternary Environments of the Soviet Union*, edited by A. A. Velichko, pp. 69–77, Addison-Wesley-Longman, Reading, Mass., 1984.

Beck, A. E., Climatically perturbed temperature gradients and their effect on regional and continental heat-flow means, *Tectonophysics*, *41*, 17–39, 1977.

Beck, A. E., G. Garven, and L. Stegena (Eds.), *Hydrogeological Regimes and Their Subsurface Thermal Effects*, *Geophys. Monogr. Ser.*, vol. 47, AGU, Washington, D. C., 1989.

Birch, F., The effects of Pleistocene climatic variations upon geothermal gradients, *Am. J. Sci.*, *246*, 729–760, 1948.

Carslaw, H. S., and J. C. Jaeger, *Conduction of Heat in Solids*, 2nd ed., 510 pp., Clarendon, Oxford, England, 1959.

Clauser, C., and H. Villinger, Analysis of conductive and convective heat transfer in a sedimentary basin, demonstrated for the Rheingraben, *Geophys. J. Int.*, *100*, 393–414, 1990.

Clauser, C., P. Giese, E. Huenges, T. Kohl, H. Lehmann, L. Rybach, J. Safanda, H. Wilhelm, K. Windloff, and G. Zoth, The thermal regime of the crystalline continental crust: Implications from the KTB, *J. Geophys. Res.*, *102*, 18,417–18,441, 1997.

Dahl-Jensen, D., K. Mosegaard, N. Gundestrip, G. D. Clow, S. J. Johnsen, A. W. Hansen, and N. Balling, Past temperatures directly from the Greenland ice sheet, *Science*, *282*, 268–271, 1998.

Drury, M. J., A. M. Jessop, and T. J. Lewis, The detection of groundwater flow by precise temperature measurements in boreholes, *Geothermics*, *13*, 163–174, 1984.

Frenzel, B., M. Pecsi, and A. A. Velichko, *Atlas of Palaeoclimates and Palaeoenvironments of the Northern Hemisphere*, *Late-Pleistocene-Holocene*, 153 pp., Gustav Fischer, Stuttgart, Germany, 1992.

Harris, R. N., and D. S. Chapman, Mid-latitude (30°–60°N) climatic warming inferred by combining borehole temperatures with surface air temperatures, *Geophys. Res. Lett.*, *28*, 747–750, 2001.

Huang, S., H. N. Pollack, and P. Y. Shen, Late Quaternary temperature changes seen in world-wide continental heat flow measurements, *Geophys. Res. Lett.*, *24*, 1947–1950, 1997.

Hurtig, E., V. Cermak, R. Haenel, and V. Zui (Eds.), *Geothermal Atlas of Europe*, 156 pp. + maps, Hermann Haack, Gotha, Germany, 1992.

Jaagus, J., Climatic fluctuations and trends in Estonia in the 20th century and possible climate change scenarios, in *Climate Change Studies in Estonia*, edited by T. Kallaste and P. Kuldna, pp. 7–12, Stockholm Environ. Inst. Tallinn Centre, Tallinn, Estonia, 1998.

Järvimäki, P., and M. Puranen, Terrestrial heat flow in Finland, in *Terrestrial Heat Flow in Europe*, edited by V. Čermak and L. Rybach, pp. 172–178, Springer-Verlag, New York, 1979.

Jessop, A. M., The distribution of glacial perturbation of heat flow in Canada, *Can. J. Earth Sci.*, *8*, 162–166, 1971.

Jõeleht, A., Geothermal studies of the Precambrian basement and Phanerozoic sedimentary cover in Estonia and Finland, Ph.D. thesis, Inst. of Geol., Univ. of Tartu, Tartu, Estonia, 1998.

Jõeleht, A., and I. T. Kukkonen, Heat flow density in Estonia—Assessment of palaeoclimatic and hydrogeological effects, *Geophysica*, *32*, 291–317, 1996.

Kohl, T., Palaeoclimatic temperature signals—Can they be washed out?, *Tectonophysics*, *291*, 225–234, 1998.

Kohl, T., and L. Rybach, Thermal and hydraulic aspects of the KTB drill site, *Geophys. J. Int.*, *124*, 756–772, 1996.

Kremenetsky, A. A., and L. N. Ovchinnikov, The Precambrian continental crust: Its structure, composition and evolution as revealed by deep drilling in the USSR, *Precambrian Res.*, *33*, 11–43, 1986.

Kukkonen, I. T., Vertical variation of apparent and palaeoclimatically corrected heat flow densities in the central Baltic Shield, *J. Geodyn.*, *8*, 33–53, 1987.

Kukkonen, I. T., Terrestrial heat flow and groundwater circulation in the bedrock in the central Baltic Shield, *Tectonophysics*, *156*, 59–74, 1988.

Kukkonen, I. T., Terrestrial heat flow and radiogenic heat production in Finland, the central Baltic Shield, *Tectonophysics*, *164*, 219–230, 1989.

Kukkonen, I. T., Thermal aspects of groundwater circulation in bedrock and its effect on crustal geothermal modelling in Finland, the central Fennoscandian Shield, *Tectonophysics*, *244*, 119–136, 1995.

Kukkonen, I. T., and P. Järvimäki, Finland, in *Geothermal Atlas of Europe*, edited by E. Hurtig, V. Cermak, R. Haenel and V. Zui, p. 29, Hermann Haack, Gotha, Germany, 1992.

Kukkonen, I. T., and C. Clauser, Simulation of heat transfer at the Kola deep-hole site—Implications for advection, heat refraction and paleoclimatic effects, *Geophys. J. Int.*, *116*, 409–420, 1994.

Kukkonen, I. T., and J. Šafanda, Palaeoclimate and structure: The most important factors controlling subsurface temperatures in crystalline rocks. A case history from Outokumpu, eastern Finland, *Geophys. J. Int.*, *126*, 101–112, 1996.

Kukkonen, I. T., I. V. Golovanova, Yu. V. Khachay, V. S. Druzhinin, A. M. Kosarev, and V. A. Schapov, Low geothermal heat flow of the Urals fold belt—Implication of low heat production, fluid circulation or palaeoclimate?, *Tectonophysics*, *276*, 63–85, 1997a.

Kukkonen, I. T., V. Glaznev, J. Jokinen, and A. Raevsky, New geothermal borehole logs in central Kola: Indication of considerable vertical variation in heat flow density, in *SVEKALAPKO, An Europrobe Project*, *2nd Workshop*, *Lammi*, *Finland*, *27–30 October*, *1997*, edited by S.-E. Hjelt, p. 49, Inst. of Geosci. and Astron., Univ. of Oulu, Oulu, Finland, 1997b.

Kukkonen, I. T., W. D. Gosnold, and J. Šafanda, Anomalously low heat flow density in eastern Karelia, Baltic Shield: A possible palaeoclimatic signature, *Tectonophysics*, *291*, 235–249, 1998.

Lewis, T. J., and A. E. Beck, Analysis of heat flow data—Detailed observations in many holes in a small area, *Tectonophysics*, *41*, 41–59, 1977.

Lunkka, J. P., M. Saarnisto, V. Gey, I. Demidov, and V. Kiselova, Extent and age of the Last Glacial maximum in the south-eastern sector of the Scandinavian Ice Sheet, *Global Planet. Change*, *31*, 407–425, 2001.

Mareschal, J.-C., F. Rolandone, and G. Bienfait, Heat flow variations in a deep borehole near Sept-Iles, Québec, Canada: Palaeoclimatic interpretation and implications for regional heat flow estimates, *Geophys. Res. Lett.*, *26*, 2049–2052, 1999.

Moiseenko, U. I., and T. Chadovich, Heat flow density data, in *Geothermal Atlas of Europe*, edited by E. Hurtig, V. Čermák, R. Haenel, and V. Zui, p. 134, Hermann Haack, Gotha, Germany, 1992.

Mosegaard, K., and A. Tarantola, Monte Carlo sampling of solutions to inverse problems, *J. Geophys. Res.*, *100*, 12,431–12,447, 1995.

NEDRA, *The Ural Super-deep Borehole (Interval 0-4008 m)*, *Geology*, *Geophysics*, *Technology* (in Russian), 205 pp., Jaroslavl, 1992.

Paterson, W. S. B., *The Physics of Glaciers*, 3rd ed., 480 pp., Elsevier Sci., New York, 1994.

Pollack, H. N., S. J. Hurter, and J. R. Johnson, Heat flow from the Earth's interior: Analysis of the global data set, *Rev. Geophys.*, *31*, 267–280, 1993.

Popov, Y. A., and V. V. Berezyn, Thermophysical and geothermal profile of the Ural super-deep hole (in Russian), in *Geotermiya Seysmichnykh i Aseysmichnyksh Zon; Sbornik Nauchnykh Trudov*, edited by V. I. Kononov, F. N. Yudakhin and V. P. Svalova, pp. 70–77, Ross. Akad. Nauk, Izdatel'stvo Nauka, Moscow, 1993.

Popov, Y. A., V. P. Pimenov, L. A. Pevzner, R. A. Romushkevich, and E. Y. Popov, Geothermal chracteristics of the Vorotilovo deep borehole drilled into the Puchezh-Katunk impact structure, *Tectonophysics*, *291*, 205–223, 1998a.

Popov, Y. A., L. A. Pevzner, and B. N. Khakhaev, Experimental geothermal investigations in superdeep wells: Method of investigations and new results, in *Proceedings of the International Conference on The Earth'sThermal Field and Related Research Methods*, edited by Y. Popov and V. Pimenov, pp. 214–218, Moscow State Geol. Prospect. Acad., Moscow, Russia, 1998b.

Popov, Y. A., L. A. Pevzner, V. P. Pimenov, and R. A. Romushkevich, New geothermal data from the Kola Superdeep well SG-3, *Tectonophysics*, *306*, 345–366, 1999a.

Popov, Y. A., R. A. Romushkevich, E. Y. Popov, K. G. Bashta, Geothermicheskiy characteristikiy razreza SG-4 (in Russian) (Geothermal char-

acteristics of profile SG-4), in *Resultatiy Bureniya i Issledovannih Uralskoy Sverghlubukoy Shkvashiny (SG-4)*, edited by B. N. Khakhaev et al., pp. 77–88, Minist. Prirodnyih RF, Jaroslavl, 1999b.

Powell, W. G., D. S. Chapman, N. Balling, and A. E. Beck, Continental heat flow density, in *Handbook of Terrestrial Heat-Flow Density Determination*, edited by R. Haenel, L. Rybach, and L. Stegena, pp. 167–222, Kluwer Acad., Norwell, Mass., 1988.

Pribnow, D., and R. Schellschmidt, Thermal tracking of upper crustal fluid flow in the Rhine Graben, *Geophys. Res. Lett.*, *27*, 1957–1960, 1998.

Sass, J. H., A. H. Lachenbruch, and A. M. Jessop, Uniform heat flow in a deep hole in the Canadian Shield and its paleoclimatic implications, *J. Geophys. Res.*, *76*, 8586–8596, 1971.

Schellschmidt, R., and R. Schulz, Hydrogeothermic stdies in the hot dry rock project at Soultz-Sous-Forêts, *Geotherm. Sci. Technol.*, *3*, 217–238, 1991.

Sen, M., and P. L. Stoffa, *Global Optimization Methods in Geophysical Inversion*, 281 pp., Elsevier Sci., New York, 1995.

Shen, P. Y., H. N. Pollack, and S. Huang, Effects of subsurface heterogeneity on the inference of climate change from borehole temperature data: Model studies and field examples from Canada, *J. Geophys. Res.*, *100*, 6383–6396, 1995.

Siegert, M. J., and J. A. Dowdeswell, Spatial variations in heat at the base of the Antarctic ice sheet from analysis of the thermal regime above subglacial lakes, *J. Glaciol.*, *42*, 501–509, 1996.

Smith, L., and D. S. Chapman, On the thermal effects of groundwater flow, 1, Regional scale systems, *J. Geophys. Res.*, *88*, 593–608, 1983.

Svendsen, J. I., et al., Maximum extent of the Eurasian ice sheets in the Barents and Kara Sea region during the Weichselian, *Boreas*, *28*, 234–242, 1999.

Tarand, A., and P. Ø. Nordli, The Tallinn temperature series reconstructed back half a millennium by use of proxy data, *Clim. Change*, *48*, 189–199, 2001.

Urban, G., and L. Tsybulia, Thermal field of the Riga Pluton, *Proc. Estonian Acad. Sci. Geol.*, *37*(2), 49–54, 1988.

Urban, G., L. Tsybulia, V. Cozel, and A. Schmidt, Geothermic characterization of the northern part of the Baltic Synecline, *Proc. Estonian Acad. Sci. Geol.*, *40*(3), 112–121, 1991.

Van der Kamp, G. and S. Bachu, Use of dimensional analysis in the study of various hydrogeological regimes, in *Hydrogeological Regimes and Their Subsurface Thermal Effects*, *Geophys. Monogr. Ser.*, vol. 47, edited by A. E. Beck, G. Garven, and L. Stegena, pp. 23–28, AGU, Washington, D. C., 1989.

Wang, K., Estimation of ground surface temperatures from borehole temperature data, *J. Geophys. Res.*, *97*, 2095–2106, 1992.

A. Jõeleht, Institute of Geology, University of Tartu, Vanemuise 46, 51014 Tartu, Estonia. (argo.joeleht@ut.ee)

I. T. Kukkonen, Geological Survey of Finland, P. O. Box 96, FIN-02151 Espoo, Finland. (ilmo.kukkonen@gsf.fi)